Research Square

Preprints are preliminary reports that have not undergone peer review.
They should not be considered conclusive, used to inform clinical practice,
or referenced by the media as validated information.

Estimation and Comparative Analysis of Daily Reference Evapotranspiration Based on Different Input Combinations and Different Models

Chaojie Niu
School of Water Conservancy Science and Engineering Zhengzhou University https://orcid.org/0000-0002-9169-3441

Xiang Li
School of Water Conservancy Science and Engineering Zhengzhou University

Chengshuai Liu
School of Water Conservancy Science and Engineering Zhengzhou University

Shan-e-hyder Soomro
School of Water Conservancy Science and Engineering Zhengzhou University

Caihong Hu (hucaihong@zzu.edu.cn)
School of Water Conservancy Science and Engineering Zhengzhou University

Research Article

Keywords: Estimation, Reference evapotranspiration, Levenberg-Marquardt, Genetic Algorithm-Back Propagation, Partial Least Squares Regression, Pearson correlation.

Posted Date: July 26th, 2021

DOI: https://doi.org/10.21203/rs.3.rs-636505/v1

License: This work is licensed under a Creative Commons Attribution 4.0 International License.
Read Full License

Estimation and comparative analysis of daily reference evapotranspiration based on different input combinations and different models

Chaojie Niu[1], Xiang Li[1], Chengshuai Liu [1], Shan-e-hyder Soomro[1], Caihong Hu[1,*]

[1]School of Water Conservancy Science and Engineering Zhengzhou University, Zhengzhou, 450001, China

202021221010285@gs.zzu.edu.cn, 20202222014305@gs.zzu.edu.cn, liucs@gs.zzu.edu.cn, shanhydersoomro110@hotmail.com, hucaihong@zzu.edu.cn

[*]Corresponding Author: Caihong Hu

Email address: hucaihong@zzu.edu.cn

Abstract

Daily reference evapotranspiration (ET_0) is the most crucial link in estimating crop water demand. In this study, Levenberg-Marquardt (L-M), Genetic Algorithm-Back Propagation (GA-BP) and Partial Least Squares Regression (PLSR) models were introduced to calculate the ET_0 values, Based on the Pearson Correlation analysis method, five meteorological factors were obtained, which were combined into six different input scenarios. Compared with the values that calculated by the the Penman Monteith (PM) formula. Root Mean Square Error (RMSE), Mean Absolute Error (MAE), Nash-Sutcliffe Efficiency (NSE), and Scatter Index (SI) were used to

evaluate the simulation performance of the models. The results showed that the simulation effect of the L-M model is better than that of the GA-BP model and PLSR model in all scenarios. PLSR model has the worst performance. The SI index of L-M6 was 46.69% lower than that of GA-BP6 and 65.78% lower than that of PLSR6. When the input factors are 3, the simulation effect of the input wind speed, the maximum temperature and the minimum temperature is the best. L-M model and GA-BP model can predict the ET_0 in the region with a lack of meteorological data. This study provides an important reference for high-precision prediction of ET_0 under different input combinations of meteorological factors.

Keywords: Estimation**,** Reference evapotranspiration, Levenberg-Marquardt, Genetic Algorithm-Back Propagation, Partial Least Squares Regression, Pearson correlation.

Introduction

As a predominantly agricultural country, China is also one of the countries lacking water resources. The problems of water ecology and water resources restrict the development of economy and society (Ding et al., 2017). Therefore, it is essential to study scientific water-saving technology and irrigation system for agricultural development (Minhas et al., 2020). Crop water demand calculation is the basis of agrarian irrigation system design and configuration of water resources in the field. The calculation of crop water requirement is the key to accurate calculation of the quantity of reference evapotranspiration (ET_0), accurately estimate the amount of reference evapotranspiration for the agriculture water resources rational allocation, real-time irrigation forecast and farmland irrigation water management plays an

important role (Shi et al., 2006). ET_0 calculation method consists of experience method, time series method, temperature method and intelligent algorithm four classes. Different procedures require different primary data in different situations. The lack of basic data will limit the use of the technique.

FAO-56 Penman Monteith method is based on water vapors diffusion theory and energy balance theory, which considers the effects of radiation and aerodynamics and the physiological characteristics of crops. The FAO-56 Penman Monteith method in regions of the world's historical meteorological data analysis reference evapotranspiration quantity ET_0 has good simulation effect. It is usually used as a standard method to calculate ET_0 (Waller and Yitayew 2016). In addition, the method also used as the standard to compare other model prediction (Shiri 2017). However, the calculation process of this method is complex, requiring more meteorological data, and it is difficult to obtain some meteorological data, so it is difficult to popularize and apply in some regions with incomplete meteorological data due to weak meteorological infrastructure (Valipour 2015). For a while, the Hargreaves and Samani method (HS) was proposed as an alternative to the PM method (Hargreaves and Samani 1985). However, it was found in many previous studies that the HS method underestimated ET_0 (Valipour 2015).

The micro weather station is a facility that can measure primary meteorological data quickly and conveniently. The increase in the number of micro weather stations provides a foundation for delivering real-time and valid meteorological data for agricultural development (Pelosi et al., 2016). However, due to facility performance,

67 the micro weather station can only collect limited meteorological data. Therefore,
68 many scholars have carried out scientific research on whether ET_0 can be predicted by
69 using less and more easily obtained meteorological data trying to find an effective
70 method to calculate ET_0 for regions with a relative lack of meteorological data
71 (Jabloun and Sahli 2008).

72 Many studies have shown that the reference evapotranspiration ET_0 has a solid
73 nonlinear relationship with meteorological factors in recent years. Therefore, methods
74 such as extensive data analysis, optimization algorithm technology have been used to
75 predict ET_0. Typical examples are evolutionary algorithms (Jing et al., 2019), Neural
76 Fuzzy Model (Malik et al., 2019), Support Vector Machines (SVM) (Ashrafzadeh et
77 al., 2020), gene programming (Mattar 2018), Extreme Learning Machine (Wu et al.,
78 2019), Random Forest Models (Shiri 2018), Deep Learning (Saggi and Jain 2019),
79 M5P Regression Tree Artificial Neural Network (ANN) (Granata 2019; Ferreira et al.,
80 2019) to conduct ET_0 modelling process. Shiri's (2017) studies have shown that the
81 machine programming model performs better than the empirical models. The
82 performance of the two-model coupling approach is superior to the performance of a
83 single model (Shiri 2018).

84 Artificial Neural Network (ANN) has strong non-linear mapping ability and
85 adaptive characteristics (Luo et al. 2015). Back Propagation (BP) neural network is a
86 mature and most used non-linear function approximation method, the BP neural
87 network is the basic principle of forwarding transfer of information and error. Back
88 Propagation can approximate any non-linear mapping in theory; thus, it can simulate

89 the climate factor and non-linear relation between the quantity of crop
90 evapotranspiration and then order to predict the amount of evapotranspiration.
91 However, the complexity of neural network structure and the need for extensive
92 sample characteristics limit the prediction accuracy of neural network. However, the
93 BP neural network algorithm has some disadvantages, such as convergence to local
94 extreme value, slow convergence operation speed, and challenging to determine the
95 number of hidden layers and hidden nodes in the calculation process. The final result
96 is quiet calculation efficiency, over-fitting results, poor prediction effect and other
97 problems (Sun et al. 2016). L-M algorithm is an improved algorithm based on BP
98 neural network. L-M algorithm is Gauss-Newton method and the combination of the
99 most vertical descent method, by adaptive adjusting damping factor to achieve
100 convergence characteristics, has higher iterative convergence speed, need not
101 calculate the Hessian matrix, at the same time with the local convergence of
102 Gauss-Newton method and the global features of the steepest descent method, In
103 many non-linear optimization problems, stable and reliable solutions are obtained.
104 On the other hand, different meteorological data are selected as the input so that
105 the forecast results will be different. Research (Yang et al. 2019) showed that
106 temperature is an essential factor affecting the accuracy of ET_0 prediction, but the
107 model's ET_0 prediction performance is significantly improved when both wind speed
108 and temperature are used as inputs. In addition, different meteorological input
109 combinations behave differently in other models. Three different models, L-M,
110 GA-BP and PLSR, were used in this study for comparative analysis and research. The

111 complexity of these three models was low, the input factors were few, the required
112 primary data were easy to obtain, and the application degree was high. Therefore, this
113 paper took Zhengzhou Station to collect conventional meteorological data and put
114 them into L-M, GA-BP and PLSR models after processing. The ET_0 prediction
115 accuracy of the three models in different input combinations is comprehensively
116 evaluated and analyzed. The research results have significant reference value for crop
117 water demand prediction and water resources management based on meteorological
118 data.

119 **Materials and method**

120 **Study region**

121 Zhengzhou is located in central China, the lower reaches of the Yellow River and
122 the north of central Henan Province, As shown in Figure 1, covering an area of 7446.2
123 km^2, between 112°42 '-114°14' E and 34°16 '-34°58' N. From 2019, there were 10.352
124 million permanent residents and 7.721 million urban residents, accounting for 74.6
125 percent of the total urban population. It has a monsoon climate in the North Temperate
126 Zone with four distinct seasons. The annual average temperature is 15.6℃. The
127 annual average rainfall is 542.15 mm. The annual sunshine time is about 1869.7
128 hours.

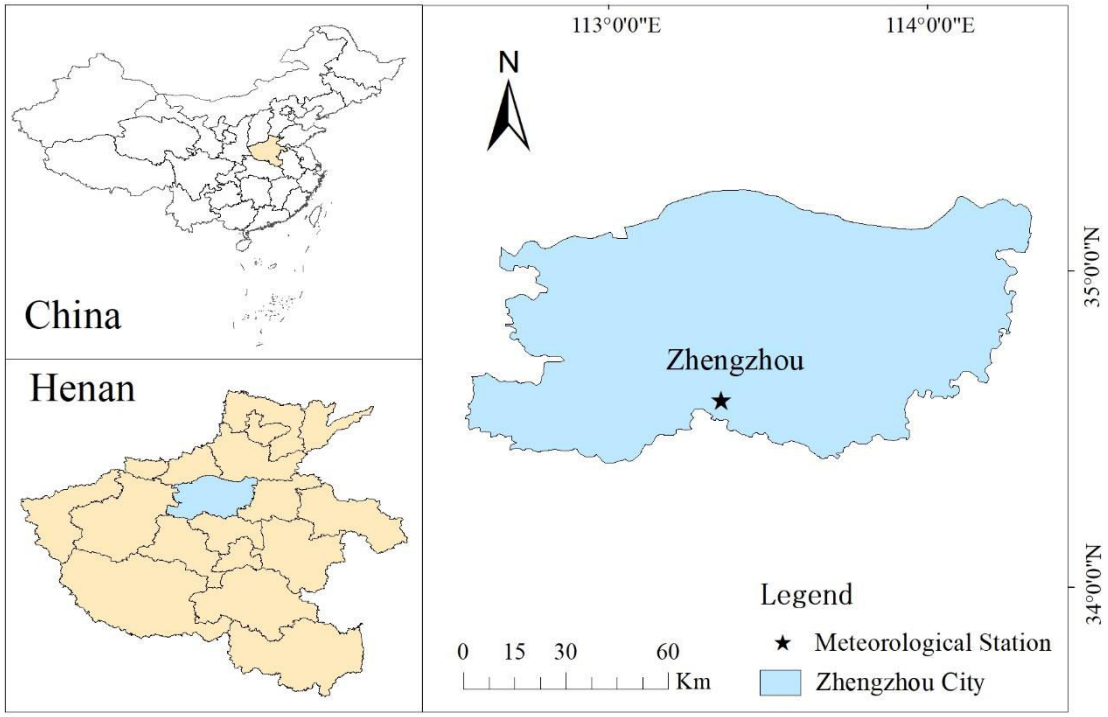

Figure1: Study area and locations of meteorological station

Data collection

The daily meteorological data for the Zhengzhou meteorological station were acquired from the China Meteorological Data Network. The data was selected during 2010–2019. These daily meteorological data include precipitation, mean relative humidity (R_H), maximum temperature (T_{max}), minimum temperature (T_{min}), solar radiation (R_a) and so on. The daily meteorological data collected (2010-2019) is separated into two datasets: the training dataset (2010-2017) and the validation dataset (2018-2019). The model parameters are trained through the training dataset, and the weights are estimated. The accuracy of the trained model is further verified by the validation dataset.

To select effective input combinations (Ruiming and Shijie 2020), Correlation analysis was used to measure the degree of correlation between the two variables. It

can delete redundant information and select the best suitable input index by using the correlation analysis method to screen the meteorological factors affecting ET_0. Pearson correlation coefficient can well represent the correlation of variables, it is calculated as：

$$Sim(S,O)=\frac{\sum_{i=1}^{n}(S_i-\bar{S})(Y_i-\bar{Y})}{\sqrt{\sum_{i=1}^{n}(S_i-\bar{S})^2}\sqrt{\sum_{i=1}^{n}(Y_i-\bar{Y})^2}} \quad (1)$$

Where, Sim(S,O): Correlation between(S,O); i: the ith sample of the indicator; n: total sample size; $\bar{S}$:average of the indicator S; $\bar{O}$:average of the indicator O.

When Sim(S,O)>0, it is the positive correlation between two indicator; Sim(S,O)<0, it is the negative correlation between two indicator; $|Sim(S,O)|\geqslant 0.8$,it means that the two variables are high correlation; $0.5\leqslant|Sim(S,O)|<0.8$; it means that the two variables are medium correlation; $|Sim(S,O)|<0.5$, it means that the two variables are low correlation. In this paper, the variables with high correlation and medium correlation are selected as the inputs of the prediction algorithm, and the results are shown in Table 1.

Table 1: Correlation of meteorological factors influencing the prediction of ET_0

Meteorological factors	T_{min}	T_{max}	R_H	SS_H	P	U_2
Correlation coefficient	0.7424	0.7920	-0.5312	0.6953	0.01453	0.5646

In this study, meteorological factors with a more significant influence on ET_0 were calculated based on Pearson correlation analysis. The results are shown in Table 1. The Pearson correlation coefficients of T_{min}, T_{max}, R_H, SS_H and U_2 are all above 0.5 (Except precipitation), which belongs to a medium and high correlation level. Besides, according to the research findings (Yang et al. 2019), the ET_0 value is greatly affected by temperature, so the temperature is a necessary input when selecting input

meteorological factors. Therefore, the above five meteorological factors are considered when determining the input composition scenario of the model. To analyze the simulation effect of different input composition scenario on ET_0 in different models, the model input composition scenario are divided into six types, as shown in Table 2. There are three input factors for scenario 1-3, 4 input factors for scenario 4-5, and 5 input factors for scenario 6. The input meteorological factors in this study are all parameters that can be easily obtained by the meteorological station, which solves the problem of backward monitoring facilities in some areas and difficult acquisition of complex parameters to a certain extent.

Table 2: Input composition scenario of the model

	T_{min}	T_{max}	R_H	SS_H	U_2
Model1	√	√	√		
Model2	√	√		√	
Model3	√	√			√
Model4	√	√		√	√
Model5	√	√	√	√	
Model6	√	√	√	√	√

Penman Monteith method

FAO-56 Penman Monteith method (Allen et al. 1998) fully considers solar radiation, energy balance, the aerodynamics and other principles. The calculation results are relatively accurate and applicable to all climates in arid and humid regions of the world. Therefore, the PM equation is recommended by FAO of United Nations to calculate ET_0 value, and the computed ET_0 value is generally used as the standard value. The equation is:

$$ET_0=\frac{0.408(R_n-G)+\gamma\frac{900}{T+273}u_2(e_s-e_a)}{\Delta+\gamma(1+0.34u_2)} \quad (2)$$

Where ET_0 is the daily potential evapotranspiration, mm/d; R_n is the net radiation, MJ/(m^2·d); G is the soil heat flux, MJ/(m^2·d), and when daily evapotranspiration is calculated, $G=0$; U_2 is the mean daily wind speed at 2m above the ground, m/s; T is the average temperature, ℃; e_s is the saturated vapor pressure, kPa; e_a is the actual vapor pressure, kPa; γ is the hygrometer constant, which is 0.065kPa/℃; Δ is the slope of the saturation vapor pressure-temperature curve, kPa / ℃.

It can be seen that in the process of using PM formula to calculate the reference evapotranspiration, a variety of parameters are involved. Many of these parameters cannot be obtained directly but need to be comprehensively calculated by other data information, including some meteorological data, geographical location dimension, altitude of the study area and additional data information. Therefore, when using this method to calculate the ET_0, it is required that the measurement equipment is complete and the measurement data meet the requirements. But the reality is that some parameters cannot be measured at all, resulting in a lack of data. Hence, it makes practical sense to use limited meteorological data as the model input to predict the reference emission.

Levenberg–Marquardt

Artificial Neural Networks (ANN) is a new intelligent information processing method that imitates the human brain to deal with problems. BP neural network algorithm is the most widely used method with the best effect. which is composed of two processes: onward transmission of information and backpropagation of error.

Through the backpropagation of error, the weight and threshold of the network are constantly adjusted to minimize the sum of squares of errors.

Neural Network algorithm also has some shortcomings in the application process, such as weight convergence to local extreme value, slow convergence speed, hidden layer and hidden nodes are difficult to determine, need a long training time, etc.

The L-M algorithm is an improved algorithm developed based on BP neural network. The procedure of the L-M algorithm is shown in Figure 2. In the algorithm, Gauss-Newton and gradient descent method are combined (Wilson and Mantooth 2013). The Gauss-Newton method is usually faster when the initial guess is relatively close to the optimal; otherwise, the gradient descent method is used to find the optimal. The parameters are automatically adjusted according to the transmitted information to achieve the convergence property without calculating the Hessian matrix during the operation. It has the local convergence property of the Gauss-Newton method and the global property of the fastest descent method (Zhao, 2002; Sun et al., 2016). Therefore, it has a higher iterative convergence speed and is widely applicable to nonlinear optimization fitting calculation L-M algorithm of the iterative formula is:

$$w^{k+1}=w^{k}+\Delta w \tag{3}$$

$$\Delta w=[J^{T}(W)J(W)+\mu I]^{-1}J^{T}(W)e_{i}(w) \tag{4}$$

Where: w is the network weights and threshold, w^{k} is The vector composed of the weights and thresholds of the *k-th* iteration, w^{k+1} is the new weight value and threshold vector, Δw is the weight increment, μ is the user-defined vector, I is the unit

matrix, $e_i(w)$ is the error, $J(w)$ is the Jacobian matrix, The Formula of Jacobian matrix is:

$$J(W)=\begin{pmatrix} \frac{\partial e_1(w)}{\partial w_1} & \cdots & \frac{\partial e_1(w)}{\partial w_n} \\ \vdots & \ddots & \vdots \\ \frac{\partial e_n(w)}{\partial w_1} & \cdots & \frac{\partial e_n(w)}{\partial w_n} \end{pmatrix} \quad (5)$$

It can be seen from Eq. 4 that μ is a tentative parameter that connects the Gauss-Newton method and gradient descent method (Sun et al., 2016). For a given μ, if they obtained Δw can reduce the error-index function $E(w)$, then μ decreases. Otherwise, μ increases. This allows the error-index function to drop to a minimum quickly.

The error index functions as:

$$E(w)=1/2n\sum_{i=1}^{n}\left\|Y_i-Y_i'\right\|^2=1/2n\sum_{i=1}^{n}e_i^2(w) \quad (6)$$

Where: Y_i is the expected network output vector, Y_i' is the actual output vector, n is the number of samples.

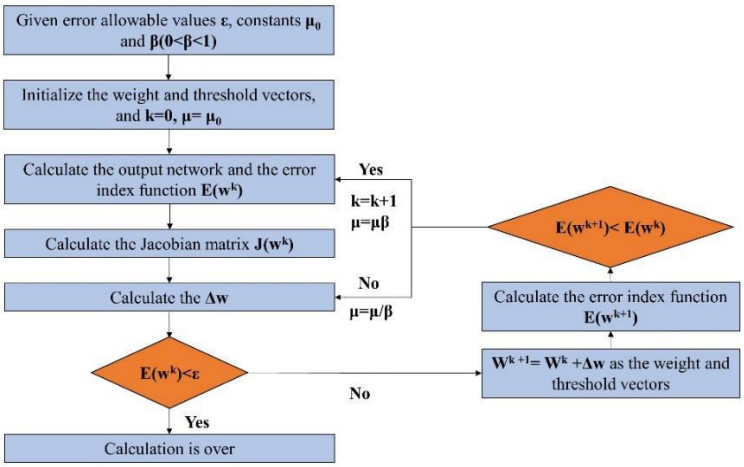

Figure 2: The procedure of the L-M algorithm

Due to significant changes in data, the sigmoid transfer function in the L-M algorithm is used this time, and the value of this function is between [0-1]. To make

241 the meteorological data conform to the model, the original meteorological information
242 is trained and predicted after normalization. After training and simulation, the
243 calculated value obtained is restored by reverse normalization, and the expected value
244 can be obtained. The normalized equation is as follows:

245 $$x_s=0.1+0.8\frac{x-x_{min}}{x_{max}-x_{min}} \quad (7)$$

246 Where, x_s represents the normalized value, x is the measured value of a factor in
247 the sample, x_{max} is the maximum value of sample data, and x_{min} is the minimum value
248 of sample data.

249 **Genetic Algorithm - Back Propagation**

250 Genetic algorithm is an iterative optimization model based on Darwinian
251 evolution theory and genetic evolution. It will be the survival of the fittest process of
252 problem-solving as chromosomes, Through the evolution of chromosomal generations,
253 the optimal or satisfactory solution of the problem is obtained. The essence of the BP
254 algorithm is to use the steepest descent method, which has the advantages of
255 simplicity, a small amount of calculation, strong parallelism, etc., However, the
256 algorithm is easy to fall into the local minimum point and runs slowly, the algorithm
257 is incomplete, network performance is poor (Liu et al., 2019). Combining BP neural
258 network and genetic algorithm, the weight and threshold of the neural network are
259 optimized by using the colony search method and that is a better overcome the
260 optimal local defect (Saleh, Ibrahim and Magdi Eiteba 2016). In this study, the simple
261 coding method is adopted to convert the initial weights and thresholds of the BP
262 neural network into chromosomes in the genetic algorithm. The encoding length is:

263 $$S=x*y+y*z+y+z \quad (8)$$

Where, x is the number of neuron nodes in the input layer, and is the number of input meteorological factors; z is the number of neuron nodes in the output layer. Since the output layer only has reference effervescent amount, $z=1$; y is the number of neuron nodes in the hidden layer.

In order to determine the random chromosome group in the genetic algorithm, the individual fitness value ξ, which is the sum of the absolute errors between the estimated value and the measured value of the training sample, is obtained through the BP neural network, as shown below:

$$\min\xi = \sum abs(k_j - o_j)$$

Where k_j is the measured value of ET_0 in the jth day, o_j is the estimated ET_0 value in the jth day.

Partial Least Squares Regression

PLSR is a standard method for linear regression modeling of multivariate data, especially when the variable data are extensive and have multiple correlations between each other. The partial least squares regression analysis model is superior to the traditional classical regression analysis method. Partial least-squares regression analysis combines the characteristics of principal component analysis, canonical correlation analysis, and linear regression analysis in the modeling process to provide some more decadent and more in-depth information in the analysis results. PLSR has also been widely applied in other disciplines (Liu et al., 2019). PLSR is essentially a linear regression analysis method, and this study introduced the PLSR model as a model comparison study. The PLSR used in the study is expressed as follows:

$$Y = X\beta + \varepsilon \tag{9}$$

Where Y is the dependent variable, X is the independent variable, β is the coefficient matrix and ε is the residual matrix.

Model performance evaluation

The following five evaluation indexes (Maroufpoor, Bozorg-Haddad and Maroufpoor 2020; Nash and Sutcliffe, 1970) were used to evaluate the performance of the model.

(1) Root mean square error (RMSE), also known as standard error; this error analysis is susceptible to reflecting the maximum or minimum error in a set of measured data. Therefore, the standard error is a good indicator of the precision of the measurement. The calculation formula is as follows:

$$\mathrm{RMSE}=\sqrt{\frac{\sum_{i=1}^{N}(S_i-O_i)^2}{N}} \tag{10}$$

(2) The IA index is used as an additional method to evaluate the model performance, and the results are in the range of 0 and 1. IA is 1, the better the simulation. The calculation formula is as follows:

$$\mathrm{IA}=1-\frac{\sum_{i=1}^{N}(S_i-O_i)^2}{\sum_{i=1}^{N}(|S_i-\bar{O}|+|O_i-\bar{O}|)^2} \tag{11}$$

(3) Mean absolute error (MAE), the mean absolute error can eliminate the interaction between the errors and objectively reflect the actual prediction error.

$$\mathrm{MAE}=\frac{\sum_{i=1}^{N}|S_i-O_i|}{N} \tag{12}$$

(4) Nash-Sutcliffe Efficiency (NSE), The Nash-Sutcliffe efficiency coefficient varies from -∞ to 1. The closer it is to 1, the closer the measured value is to the

simulated value. A value of 0 indicates that the model's simulation results are the same as the mean value of the measured values. A value less than zero indicate that the measured mean value is better than the simulated value. The calculation formula is as follows:

$$NSE=1-\frac{\sum_{i=1}^{N}(S_i-O_i)^2}{\sum_{i=1}^{N}(O_i-\bar{O})^2} \quad (13)$$

(5) Scatter index (SI) is a parameter used to evaluate the performance of the model; in this study, the SI was divided into four ranges to evaluate the model performance. Excellent when SI < 0.1, good if 0.1 < SI < 0.2, fair if 0.2 < SI < 0.3, and poor if SI > 0.3. The calculation formula is as follows:

$$SI=\frac{RMSE}{\bar{O}}=\frac{\sqrt{1/N\sum_{i=1}^{N}(S_i-O_i)^2}}{\bar{O}} \quad (14)$$

In the above formula, N is the number of samples, S_i is the forecasted value of ET_0 on day i, O_i is the observed value of ET_0 on day i, and $\bar{O}$ is the average of the measured value of ET_0.

Results

Performance evaluation of model

L-M model and GA-BP model are both algorithms based on neural network, which contain input layer, hidden layer, and output layer in the process of machine learning. The number of the input layer and output layer is relatively easy to determine, and the number of the hidden layer is a very important factor in the operation process, which depends on the type and number of input (Faris, Mirjalili and Aljarah 2019). Improper selection of hidden layers will not only affect the efficiency of machine learning but also directly affect the simulation results. It is

found that the more hidden layers, the better the calculation effect is, and there is no specific rule to determine the number of hidden layers in many research works of literature (Kanellopoulos and Wilkinson 1997). In this study, the number of neurons in the hidden layer was determined through trial and error to ensure the simulation effect, operation efficiency, and stability of the model. L-M model and GA-BP model adopt the same input structure. For example, 3-6-1 means that the input layer has 3 (meteorological factors), the number of neurons in the hidden layer is 6, and the output layer is 1 (ET_0). It is worth noting that the L-M model and GA-BP model have different iteration types, so the number of iterations is also different. It is found that when the number of iterations reaches a certain number, increasing the number of iterations has little effect on improving the simulation accuracy of the model and even increases the operating burden of the model. Through experiments, the number of iterations of the L-M model is 1500, and the number of iterations of GA-BP is 10.

The six input scenarios were put into three different models, namely L-M, GA-BP, and PLSR. The performance comparison analysis results of predicted ET_0 results and PM formula calculation results are shown in Table 3. The simulation accuracy of the same model increases with the increase of input factors on the whole, and they all reach the maximum when the input factors are 5. The simulation accuracy of different models from high to bottom is L-M, GA-BP, PLSR.

Table 3: Statistical performance of the L-M, GA-BP and PLSR models.

Model	Structure	Training (2010-2017)				validating (2018-2019)			
		RMSE	IA	MAE	NSE	RMSE	IA	MAE	NSE

L-M 1	3-6-1	0.5143	0.9724	0.3743	0.8977	0.5327	0.9693	0.3978	0.8832
L-M 2	3-6-1	0.4841	0.9769	0.3599	0.9128	0.4297	0.9801	0.3352	0.9240
L-M 3	3-6-1	0.4840	0.9771	0.3516	0.9138	0.4209	0.9810	0.3300	0.9271
L-M 4	4-8-1	0.3064	0.9899	0.2167	0.9604	0.2897	0.9915	0.2175	0.9655
L-M 5	4-8-1	0.4009	0.9831	0.3104	0.9321	0.3647	0.9866	0.2910	0.9452
L-M 6	5-10-1	0.1857	0.9964	0.1970	0.9854	0.1397	0.9980	0.1845	0.9920
GA-BP 1	3-6-1	0.4960	0.9717	0.3626	0.8953	0.5597	0.9664	0.4027	0.8710
GA-BP 2	3-6-1	0.4803	0.9745	0.3560	0.9048	0.4557	0.9775	0.3431	0.9145
GA-BP 3	3-6-1	0.4800	0.9745	0.3552	0.9049	0.4531	0.9778	0.3418	0.9155
GA-BP 4	4-8-1	0.3580	0.9850	0.2622	0.9459	0.3397	0.9873	0.2540	0.9525
GA-BP 5	4-8-1	0.4010	0.9807	0.2995	0.9321	0.4099	0.9803	0.3161	0.9308
GA-BP 6	5-10-1	0.3013	0.9891	0.2278	0.9617	0.2622	0.9921	0.2087	0.9717
PLSR 1	--	0.6998	0.9406	0.5669	0.7944	0.6979	0.9416	0.5822	0.7795
PLSR 2	--	0.9297	0.8826	0.7500	0.6325	0.9354	0.8832	0.7606	0.6399
PLSR 3	--	0.6991	0.9511	0.5500	0.7957	0.6969	0.9509	0.5727	0.7886
PLSR 4	--	0.4730	0.9756	0.3611	0.9056	0.4710	0.9765	0.3574	0.9087
PLSR 5	--	0.6331	0.9602	0.5123	0.8308	0.6412	0.9609	0.5210	0.8308
PLSR 6	--	0.4267	0.9811	0.3166	0.9232	0.4084	0.9829	0.3015	0.9313

Table.3 This shows that when the input meteorological factor for three, the prediction effect of scenario 3 in different models is better than that of scenario 1 and 2, scenario 3 and 2 in L-M and GA-BP model is better than that of scenario 1, the RMSE was 0.4209mm and 0.4297mm, respectively, and MAE was 0.33 mm, 0.3352 mm, the efficiency of the evaluation model to simulate index IA was 0.9810, 0.9801, NSE was 0.9271 and 0.9240. In the PLSR model, Scenario 3 is still the best, but the simulation effect of scenario 1 is better than scenario 2. Figure 3 shows the simulated values of ET_0 of L-M, GA-BP, and PLSR models and the calculated values of the PM formula, respectively, in scenarios 1-3. Under the same input scenario, the L-M model

has the best ET_0 prediction effect. PLSR model has a poor prediction effect, which PLSR2 model has the worst simulation effect, and the correlation coefficient R^2 was only 0.6463, which decreased by 30.17% compared with L-M2 (R^2=0.9255) and 29.42% compared with GA-BP2 (R^2=0.9157).

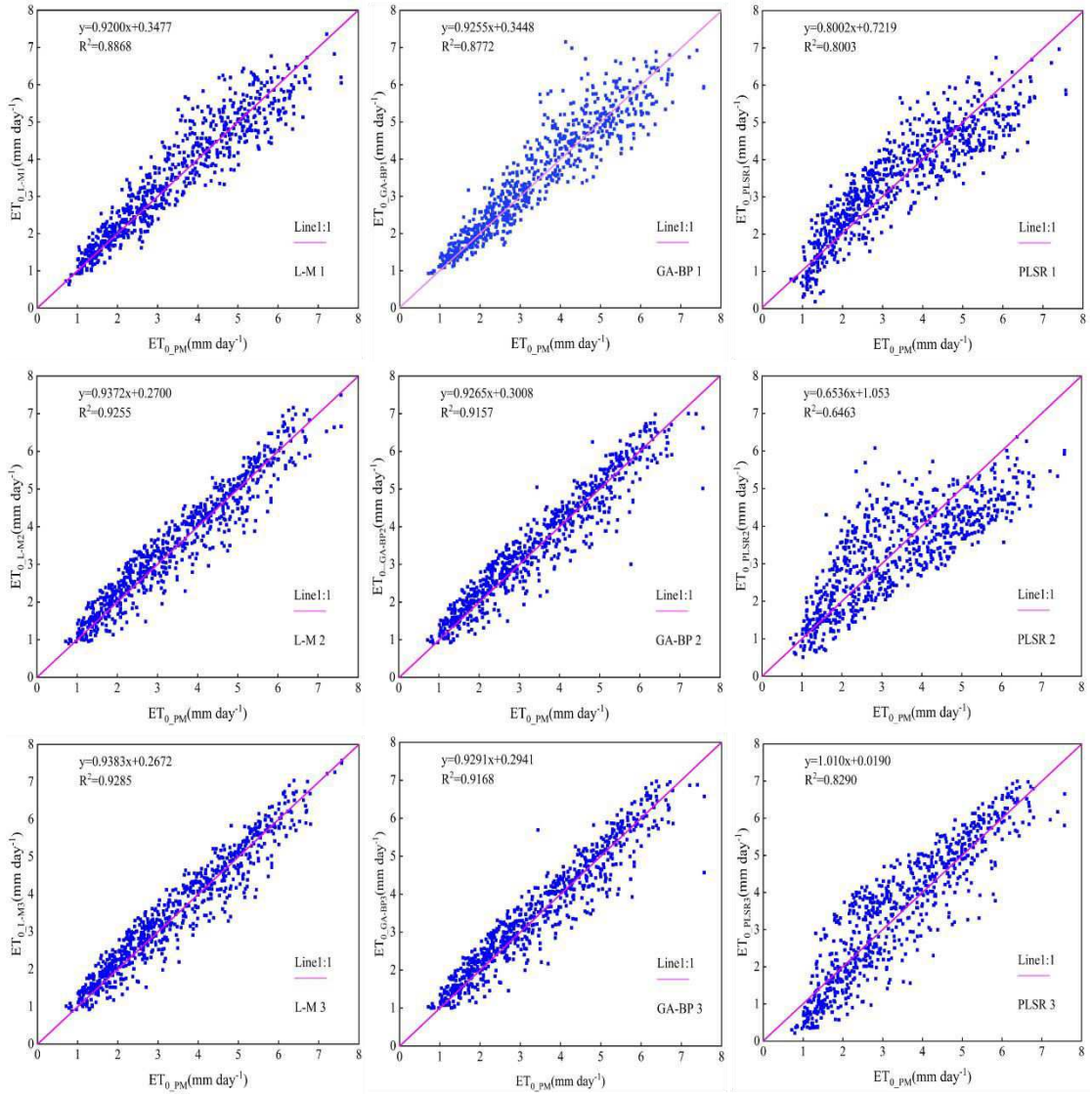

Figure 3: Predicted values of scenario 1-3 in L-M, GA-BP, PLSR models and calculated values of PM method

Four input factors of Scenario 4-5 were put into the three models, and the results showed that Scenario 4 had the best simulation effect. In the same model, The IA index of scenario 4 was 0.49%, 0.71%, and 1.60% higher than that of scenario 5,

respectively. The growth rate of the IA index from small to large was L-M<GA-BP<PLSR, Since the IA index is used to evaluate the performance of the model, and the results are in the range of 0 and 1. IA is 1, the better the simulation. On the other hand, it also shows that the simulation effect of the L-M model is better than that of GA-BP and PLSR. Comparison results of Scenario 4 among different models showed that RMSE of L-M4 (0.2897mm) was 14.72% lower than that of GA-BP4 (0.3397mm) and 38.49% lower than that of PLSR4 (0.4710mm). Similarly, for NSE, L-M4 increased by 1.35% and 5.88% respectively compared with GA-BP4 and PLSR4. Figure 4 shows the simulated values of ET_0 of L-M, GA-BP, and PLSR models and the calculated values of the PM formula in Scenario 4-5, respectively. It can be seen that L-M4 is the most consistent with the 1:1 line (y = x) (Kotz et al., 1982) with a high degree of the fitting. In addition, the scatter pattern of the GA-BP model tends to sag to the upper left, and the scatter pattern of the PLSR model tends to sag to the lower right. It can be clearly seen from Figure 3 and Figure 4 that under the same other input conditions, the input scenario with wind speed as the input meteorological factor has a better simulation effect, indicating that wind speed has a greater impact on the estimation of ET_0.

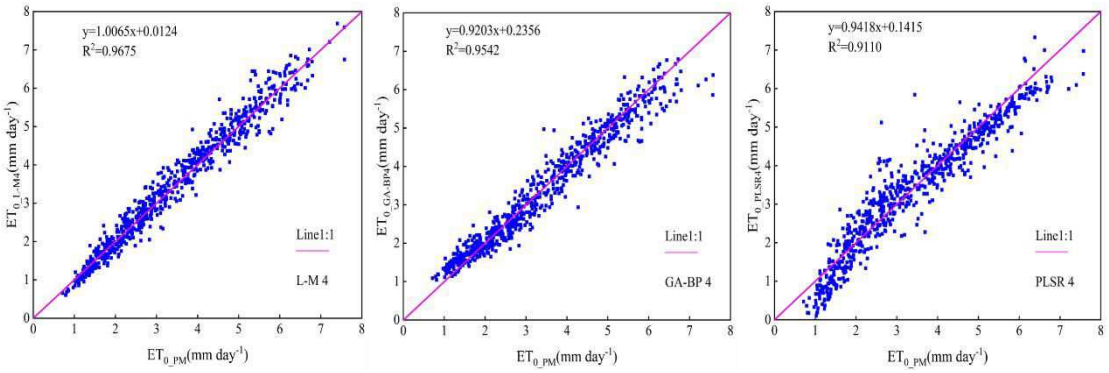

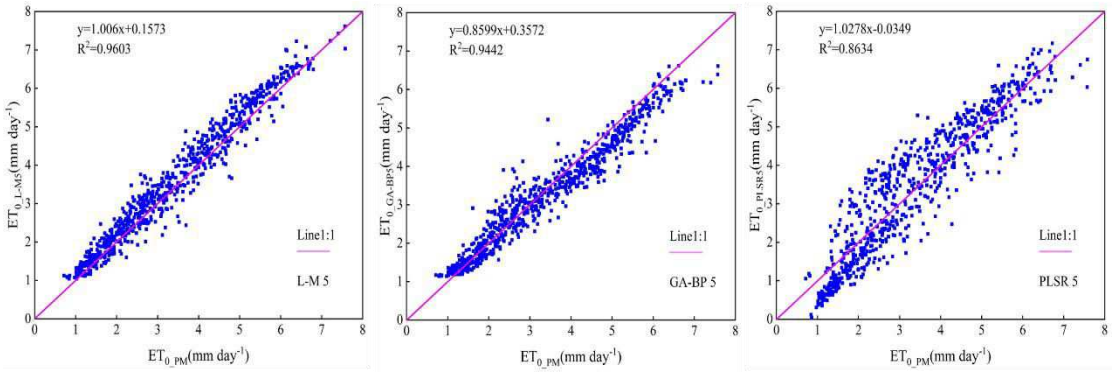

388

389 Figure 4: Predicted values of scenario 4-5 in L-M, GA-BP, PLSR models and

390 calculated values of PM method

391 Figure 5 shows the simulated values of ET_0 of L-M, GA-BP, and PLSR models

392 and the calculated values of the PM formula in Scenario 6. As shown in the figure,

393 L-M6 is more consistent with the 1:1 line (y = x) and the correlation coefficient

394 R^2=0.9925. It is worth noting that the R^2 of GA-BP6 and PLSR6 are also significantly

395 increased, which are 0.9818 and 0.9349, respectively. The two models have a more

396 obvious trend of sag in the upper left and lower right scatter plots, which is related to

397 the simulation accuracy of the model.

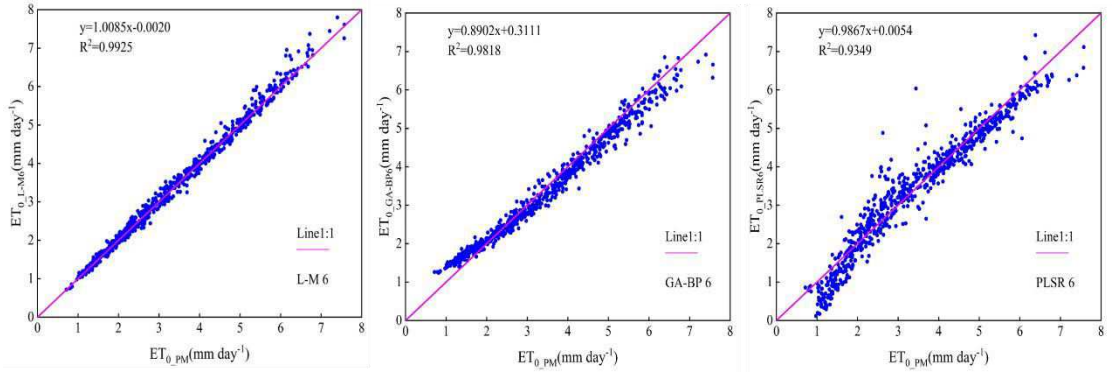

398

399 Figure 5: Predicted values of scenario 6 in L-M, GA-BP, PLSR models and calculated

400 values of PM method

401 It can also be seen from Table 3 that scenario 6 has the best simulation effect in

402 each model. RMSE and MAE, which represent model simulation error in L-M6, are

403 0.1397mm and 0.1845mm, respectively, which are 46.72%, 11.60%, 65.79%, and
404 38.81% lower than those in GA-BP6 and PLSR6, respectively. Similarly, the indexes
405 IA and NSE representing the model stability and simulation efficiency are 0.9980 and
406 0.9920, respectively. Compared with the other two models, the improvement was
407 0.61%, 2.1%, and 1.51%, 6.12%, respectively. All the indicators have improved
408 significantly.

409 **Comparison of the models**

410 Figure 6 shows the simulation renderings of the daily ET_0 simulated values and
411 the daily ET_0 calculated values obtained by the PM formula in the validation time
412 series of Scenario 6. ET_0 and PM calculated by different models have the same overall
413 trend of change. ET_0 values show a single peak every year. From April to September,
414 the temperature is relatively high, and the sunshine hours are sufficient, so the ET_0
415 value is large; from October to December and January to March, the temperature is
416 low, and the sunshine hours are short, so the ET_0 value is small. The predicted daily
417 ET_0 value of L-M6 is basically the same as the standard value calculated by the PM
418 formula. The predicted ET_0 value of GA-BP6 from November to February of each
419 year is larger than the standard value, and the predicted ET_0 value from March to
420 October is smaller than the standard value. For PLSR6, the predicted ET_0 value is
421 smaller than the standard value on the whole, and the performance is more significant
422 from November to February of the next year.

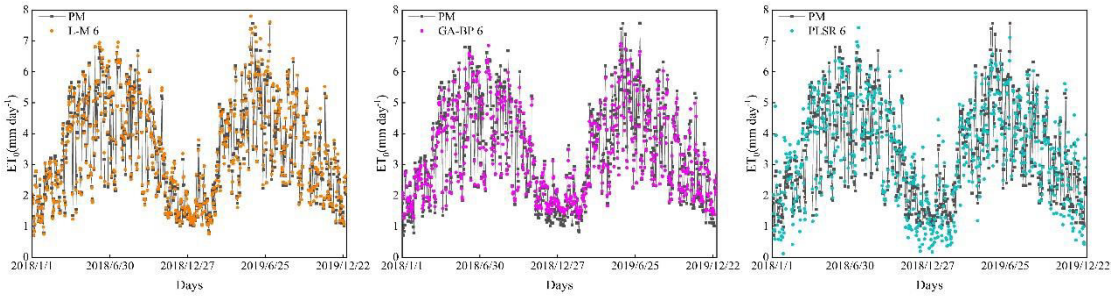

Figure 6: Comparison of scenario 6 daily ET_0 from the L-M GA-BP PLSR model with the calculated daily ET_0 using the PM method.

The Scatter Index (SI) is a parameter used to evaluate the model performance. When SI<0.1, the model performance is excellent, 0.1<SI<0.2, the model performance is good, 0.2<SI<0.3, the model performance is normal, and SI>0.3, the model performance is poor. According to Table 4, only L-M4, L-M6, GA-BP4, and GA-BP6 have SI values less than 0.1 in the validation dataset.

Table 4: SI values for different input combinations in different models

Model	Structure	Training (2010-2017)	validating (2018-2019)
		SI	SI
L-M 1	3-6-1	0.1472	0.1567
L-M 2	3-6-1	0.1359	0.1264
L-M 3	3-6-1	0.1355	0.1238
L-M 4	4-8-1	0.0917	0.0852
L-M 5	4-8-1	0.1200	0.1073
L-M 6	5-10-1	0.0556	0.0411
GA-BP 1	3-6-1	0.1490	0.1646
GA-BP 2	3-6-1	0.1421	0.1340
GA-BP 3	3-6-1	0.1419	0.1333
GA-BP 4	4-8-1	0.1072	0.0999
GA-BP 5	4-8-1	0.1201	0.1206

GA-BP 6	5-10-1	0.0902	0.0771
PLSR 1	--	0.2087	0.2153
PLSR 2	--	0.2790	0.2751
PLSR 3	--	0.2081	0.2108
PLSR 4	--	0.1416	0.1385
PLSR 5	--	0.1896	0.1886
PLSR 6	--	0.1277	0.1201

It can be intuitively seen from Figure 7 that PLSR2 had the worst simulation performance, while L-M6 had the best simulation performance, and compared with GA-BP6 and PLSR6, the SI value increased by 46.69% and 65.78%.

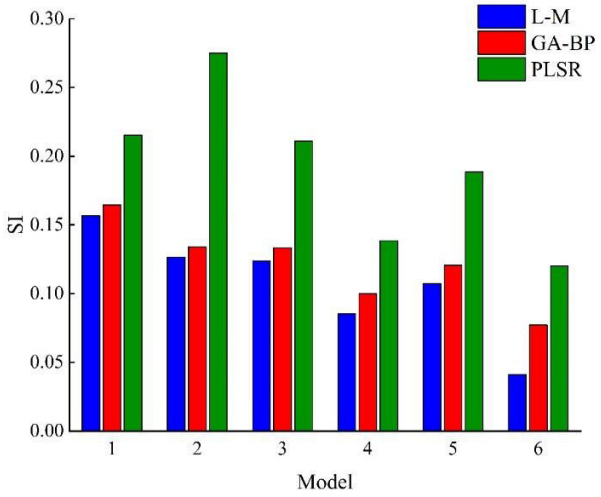

Figure 7: SI values for different scenarios of models.

The highest accuracy was all scenarios 6 of L-M GA-BP and PLSR models. The residuals (estimated errors) of the L-M6, GA-BP6, and PLSR6 models were analyzed using a boxplot (Figure 8).

A boxplot is a statistical graph showing a set of data dispersion. It is mainly used to reflect the distribution characteristics of original data and can also compare the distribution characteristics of multiple groups of data. The boxplot is displayed based

on an error distribution of four values (Maroufpoor et al. 2020 Seyedzadeh et al. 2020) which are the first quartile (Q1), the third quartile (Q3), the interquartile range (IQR), and the portion of the rectangle showing the median. This is shown in Figure 8. The most important thing in the box chart is the calculation of relevant statistical points, which can be achieved by percentile calculation. Among them, Q3 is more important than Q1 in error judgment of data distribution because Q3 covers 75% of errors, while Q1 only covers 25% of errors. As can be seen from the figure, the Q1 of L-M6 is −0.0917, which is better than that of GA-BP6 (Q1 =−0.1110) and PLSR6 (Q1 =−0.1602). L-M6 with a difference of ΔQ3 = 0.0193 (compared with GA-BP6) and ΔQ3 = 0.0685 (compared to PLSR6) has higher accuracy in performance. In L-M6, IQR is smaller than the other two models, indicating that the error distribution is near zero.

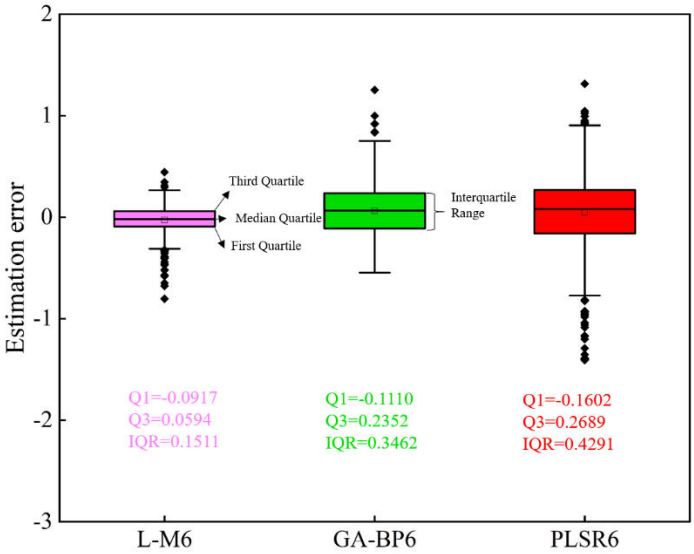

Figure 8: Boxplot of estimation error in estimating ET_0 by L-M6 GA-BP6 and PLSR6.

Conclusion and Discussion

Daily Reference evapotranspiration (ET_0) as the key part of crop water requirement calculation in modern agriculture, an accurate calculation to provide support for better planning and management of water resources, as a result of international Food and Agriculture Organization promoted the PM method in the calculating process needs more meteorological data, some data is difficult to measure, popularized in data lack of area is difficult to apply, and the whole calculation process is more complicated. In order to solve this problem, L-M, GA-BP and PLSR models were introduced in this study. The historical meteorological data of Zhengzhou station from 2010 to 2019 were used for the data. Based on Pearson correlation analysis method, five meteorological factors were obtained, which were combined into six different input scenarios. In six input scenarios, RMSE, MAE, IA, and NSE, SI was used to predict the results, and the daily ET_0 calculated by the PM method was combined to evaluate the performance of ET_0 predicted by these three models. The results showed that:

(1) The prediction accuracy of the L-M model in any input scenario is better than that of the other two models.

(2) When more meteorological parameters were input, the prediction accuracy of the three models was improved. When scenario 6 was input, the simulation accuracy of the three models reached the maximum, and the L-M model's determination coefficient (R^2=0.9925) was 5.8% higher than the PLSR's determination coefficient (R^2=0.9349).

(3) When the input meteorological factors are three, T_{min} and T_{max} are fixed input factors, and R_H, SSH, and U_2 are added, respectively, the accuracy of ET_0 prediction by L-M and GA-BP models increases successively. Moreover, the accuracy of the L-M model and GA-BP model is close when the SSH is input and the U_2. For the PLSR model, the simulation accuracy is the worst when the SSH is input, and the determination coefficient R^2 is only 0.6463. When U_2 is input, the simulation accuracy is still the best. It can be seen that: 1) when the input weather factors are three, the input scenario containing U_2 has the best simulation accuracy among the three models. 2) When input SSH and U_2, the simulation accuracy of L-M and GA-BP models is close, and the appropriate input combination can be selected according to the regional data type. 3) PLSR model is not sensitive to SSH, and its overall prediction effect is inferior to the other two models.

(4) As the model was tested by historical meteorological data in the temperate climate zone of the middle reaches of the Yellow River, it could represent the simulation effect of a certain region. As the global climate is changeable, the model may be inaccurate under different climate change conditions, so it cannot be directly used in other climate zones in the world. When the model in this study is applied to other climatic regions, it is recommended to conduct a systematic evaluation before application. In addition, we can also consider setting up multiple micro weather stations under different climate conditions to collect more real-time and accurate data to improve the reliability of the model.

Authors Contributions

For this research paper with several authors, a short paragraph specifying their individual contributions was provided. Chaojie Niu developed the original idea and contributed to the research design for the study. Xiang Li and Chengshuai Liu were responsible for data collection and charting. Shan-e-hyder Soomro provided some guidance for the writing of the article. Caihong Hu provided guidance and improving suggestion. All authors have read and approved the final manuscript.

Funding

This work was funded by Projects of National Natural Science Foundation of China, grant number (51979250), Key projects of National Natural Science Foundation of China (51739009), National key research and development projects(2019YFC1510703) and Key Research and Promotion Projects (technological development) in Henan Province (202102310587).

Declaration of competing interest

The authors declare that there is no conflict of interest regarding the publication of this paper.

Availability of data and material

Not applicable.

References

Allen, R.G., Pereira, L.S., Raes, D., Smith, M. (1998) Crop Evapotranspiration-guidelines for Computing Crop Water Requirements. FAO Irrigation and Drainage Paper 56. Food and Agriculture Organization of the United Nations, Rome, Italy.

Ashrafzadeh, A., Kişi, O., Aghelpour, P., Biazar, S. M. & Masouleh, M. A. (2020) Comparative Study of Time Series Models, Support Vector Machines, and GMDH in Forecasting Long-Term Evapotranspiration Rates in Northern Iran. Journal of Irrigation and Drainage Engineering 146, https://doi:10.1061/(asce)ir.1943-4774.0001471.

Ding, Y., Wang W., Song R., Shao Q., Jiao X. & Xing W. (2017) Modeling spatial and temporal variability of the impact of climate change on rice irrigation water requirements in the middle and lower reaches of the Yangtze River, China. Agricultural Water Management, 193, 89-101. https://doi:10.1016/j.agwat.2017.08.008

Faris, H., Mirjalili S. & Aljarah I. (2019) Automatic selection of hidden neurons and weights in neural networks using grey wolf optimizer based on a hybrid encoding scheme. International Journal of Machine Learning and Cybernetics, 10, 2901-2920. https://doi:10.1007/s13042-018-00913-2

Ferreira, L. B., da Cunha, F. F., de Oliveira, R. A. & Fernandes Filho, E. I. (2019) Estimation of reference evapotranspiration in Brazil with limited meteorological data using ANN and SVM – A new approach. Journal of Hydrology 572,556-570, https://doi:10.1016/j.jhydrol.2019.03.028.

Granata, F. (2019) Evapotranspiration evaluation models based on machine learning algorithms—A comparative study. Agricultural Water Management, 217, 303-315.

https://doi:10.1016/j.agwat.2019.03.015

Hargreaves, G.H., Samani, Z.A. (1985) Reference crop evapotranspiration from temperature. Appl. Eng. Agric. 1 (2), 96–99. https://doi:10.13031/2013.26773

Jabloun, M. & Sahli A. (2008) Evaluation of FAO-56 methodology for estimating reference evapotranspiration using limited climatic data. Agricultural Water Management, 95, 707-715. https://doi:10.1016/j.agwat.2008.01.009

Jing, W., et al. (2019) Implementation of evolutionary computing models for reference evapotranspiration modeling: short review, assessment and possible future research directions. Engineering Applications of Computational Fluid Mechanics, 13, 811-823. https://doi:10.1080/19942060.2019.1645045

Kanellopoulos, I. & Wilkinson G. G. (1997) Strategies and best practice for neural network image classification. International Journal of Remote Sensing, 18, 711-25. https://doi:10.1080/014311697218719

Kotz, S., Johnson, H.L., Read, C.B. (1982) Encyclopedia of statistical sciences. https://doi:10.4249/scholarpedia.2658

Liu, S., Peng Y., Xia Z., Hu Y., Wang G., Zhu A. X. & Liu Z. (2019) The GA-BPNN-Based Evaluation of Cultivated Land Quality in the PSR Framework Using Gaofen-1 Satellite Data. Sensors (Basel), 19. https://doi:10.3390/s19235127

Luo, Y., Traore S., Lyu X., Wang W., Wang Y., Xie Y., Jiao X. & Fipps G. (2015) Medium Range Daily Reference Evapotranspiration Forecasting by Using ANN and Public Weather Forecasts. Water Resources Management, 29, 3863-3876. https://doi:10.1007/s11269-015-1033-8

564 Malik, A., Kumar A., Ghorbani M. A., Kashani M. H., Kisi O. & Kim S. (2019) The viability of
565 co-active fuzzy inference system model for monthly reference evapotranspiration estimation:
566 case study of Uttarakhand State. Hydrology Research, 50, 1623-1644.
567 https://doi:10.2166/nh.2019.059
568 Maroufpoor, S., Bozorg-Haddad O. & Maroufpoor E. (2020) Reference evapotranspiration
569 estimating based on optimal input combination and hybrid artificial intelligent model:
570 Hybridization of artificial neural network with grey wolf optimizer algorithm. Journal of
571 Hydrology, 588. https://doi:10.1016/j.jhydrol.2020.125060
572 Mattar, M. A. (2018) Using gene expression programming in monthly reference
573 evapotranspiration modeling: A case study in Egypt. Agricultural Water Management, 198,
574 28-38. https://doi:10.1016/j.agwat.2017.12.017
575 Minhas, P. S., Ramos T. B., Ben-Gal A. & Pereira L. S. (2020) Coping with salinity in irrigated
576 agriculture: Crop evapotranspiration and water management issues. Agricultural Water
577 Management, 227. https://doi:10.1016/j.agwat.2019.105832
578 Nash, J.E., Sutcliffe, J.V. (1970). River flow forecasting through conceptual models part: I a
579 discussion of principles. J. Hydrol. 10 (3), 282–290.
580 https://doi:10.1016/0022-1694(70)90255-6
581 Pelosi, A., Medina H., Villani P., D'Urso G. & Chirico G. B. (2016) Probabilistic forecasting of
582 reference evapotranspiration with a limited area ensemble prediction system. Agricultural
583 Water Management, 178, 106-118. https://doi:10.1016/j.agwat.2016.09.015
584 Ruiming, F. & S. Shijie (2020) Daily reference evapotranspiration prediction of Tieguanyin tea
585 plants based on mathematical morphology clustering and improved generalized regression

586 neural network. Agricultural Water Management, 236.
587 https://doi:10.1016/j.agwat.2020.106177
588 Saggi, M. K. & Jain S. (2019) Reference evapotranspiration estimation and modeling of the
589 Punjab Northern India using deep learning. Computers and Electronics in Agriculture, 156,
590 387-398. https://doi:10.1016/j.compag.2018.11.031
591 Saleh, S. M., Ibrahim K. H. & Magdi Eiteba M. B. (2016) Study of genetic algorithm performance
592 through design of multi-step LC compensator for time-varying nonlinear loads. Applied Soft
593 Computing, 48, 535-545. https://doi:10.1016/j.asoc.2016.07.043
594 Seyedzadeh, A., Maroufpoor S., Maroufpoor E., Shiri J., Bozorg-Haddad O. & Gavazi F. (2020)
595 Artificial intelligence approach to estimate discharge of drip tape irrigation based on
596 temperature and pressure. Agricultural Water Management, 228.
597 https://doi:10.1016/j.agwat.2019.105905
598 Shi Xiaonan, Wang Quanjiu, Wang Xin, et al. (2006) Adaptability of different reference
599 evapo-transpiration estimation methods in Xinjiang region[J]. Transactions of the Chinese
600 Society of Agricultural Engineering, 22(6): 19-23.
601 Shiri, J. (2017) Evaluation of FAO56-PM, empirical, semi-empirical and gene expression
602 programming approaches for estimating daily reference evapotranspiration in hyper-arid
603 regions of Iran. Agricultural Water Management, 188, 101-114.
604 https://doi:10.1016/j.agwat.2017.04.009
605 Shiri, J. (2018) Improving the performance of the mass transfer-based reference
606 evapotranspiration estimation approaches through a coupled wavelet-random forest
607 methodology. Journal of Hydrology, 561, 737-750. https://doi:10.1016/j.jhydrol.2018.04.042

608 Sun Weipeng, Chen Gang, Gu Shixiang (2016) Real-time prediction of reference crop
609 evapotranspiration based on L-M neural network algorithm [J]. Journal of Irrigation and
610 Drainage, 35(S1):112-115.
611 Valipour, M. (2015) Temperature analysis of reference evapotranspiration models. Meteorological
612 Applications, 22, 385-394. https://doi:10.1002/met.1465
613 Waller, P., Yitayew, M. (2016) Crop evapotranspiration[M] Irrigation and Drainage Engineering.
614 Cham: Springer International Publishing, 89-104. https://doi:10.1007/978-3-319-05699-9
615 Wilson, P. & Mantooth H. A. (2013) Model-Based Optimization Techniques. In Model-Based
616 Engineering for Complex Electronic Systems, 347-367. ISBN：9780123850850
617 Wu, L., Zhou H., Ma X., Fan J. & Zhang F. (2019) Daily reference evapotranspiration prediction
618 based on hybridized extreme learning machine model with bio-inspired optimization
619 algorithms: Application in contrasting climates of China. Journal of Hydrology, 577.
620 https://doi:10.1016/j.jhydrol.2019.123960
621 Yang, Y., Cui, Y., Bai, K., Luo, T., Dai, J., Wang, W., Luo, Y. (2019) Short-term forecasting of
622 daily reference evapotranspiration using the reduced-set Penman-Monteith model and public
623 weather forecasts. Agric. Water Manag. 211, 70–80. https://doi:10.1016/j.agwat.2018.09.036
624 Zhao H, Zhou R, Lin T. (2002) Neural Network Supervisory and Control Based on
625 Levenberg-Marquardt Algorithm. Journal of Xi'an Jiaotong University, 36(05):523-527.
626 https://doi:10.1002/mop.10502